EXPERIMENTAL DETERMINATION OF CONVECTIVE HEAT TRANSFER COEFFICIENT IN WIRE ELECTRO DISCHARGE MACHINING

NADIAH WAZNAH BINTI ZABIDI

UNIVERSITI MALAYSIA PAHANG

UNIVERSITI MALAYSIA PAHANG

BORANG PENGESAHAN STATUS TESIS ◆

JUDUL: **EXPERIMENTAL DETERMINATION OF CONVECTIVE HEAT TRANSFER COEFFICIENT IN WIRE ELECTRO DISCHARGE MACHINING**

SESI PENGAJIAN: 2008/2009

Saya **NADIAH WAZNAH BINTI ZABIDI (860821-56-6088)**
(HURUF BESAR)

mengaku membenarkan tesis (Sarjana Muda / ~~Sarjana / Doktor Falsafah~~)* ini disimpan di perpustakaan dengan syarat-syarat kegunaan seperti berikut:

1. Tesis ini adalah hakmilik Universiti Malaysia Pahang (UMP).
2. Perpustakaan dibenarkan membuat salinan untuk tujuan pengajian sahaja.
3. Perpustakaan dibenarkan membuat salinan tesis ini sebagai bahan pertukaran antara institusi pengajian tinggi.
4. **Sila tandakan (√)

	SULIT	(Mengandungi maklumat yang berdarjah keselamatan atau kepentingan Malaysia seperti yang termaktub di dalam AKTA RAHSIA RASMI 1972)
	TERHAD	(Mengandungi maklumat TERHAD yang telah ditentukan oleh organisasi / badan di mana penyelidikan dijalankan)
√	**TIDAK TERHAD**	

Disahkan oleh:

(TANDATANGAN PENULIS)	(TANDATANGAN PENYELIA)
Alamat Tetap: **B 08-13A CENGAL CONDOMINIUM** **BANDAR SRI PERMAISURI** **56000 CHERAS KUALA LUMPUR**	Nama Penyelia **MDM MAS AYU BT HASSAN**
Tarikh:	Tarikh:

CATATAN: * Potong yang tidak berkenaan
** Jika tesis ini SULIT atau TERHAD, sila lampirkan surat daripada pihak berkuasa/organisasi berkenaan dengan menyatakan sekali tempoh tesis ini perlu dikelaskan sebagai SULIT atau TERHAD.
◆ Tesis dimaksudkan sebagai tesis bagi Ijazah Doktor Falsafah dan Sarjana secara Penyelidikan, atau disertasi bagi pengajian secara kerja kursus dan penyelidikan, atau Laporan Projek Sarjana Muda (PSM).

EXPERIMENTAL DETERMINATION OF CONVECTIVE HEAT TRANSFER COEFFICIENT IN WIRE ELECTRO DISCHARGE MACHINING

NADIAH WAZNAH BINTI ZABIDI

A report submitted in partial fulfilment of the requirements
for the award of the degree of
Bachelor of Mechanical Engineering

Faculty of Mechanical Engineering
UNIVERSITI MALAYSIA PAHANG

NOVEMBER 2008

SUPERVISOR'S DECLARATION

We hereby declare that we have checked this project and in our opinion this project is satisfactory in terms of scope and quality for the award of the degree of Bachelor of Mechanical Engineering

Signature : …………………………..
Name of Supervisor :
Position :
Date :

Signature : ………………………….
Name of Panel :
Position :
Date :

STUDENT'S DECLARATION

I hereby declare that the work in this thesis is my own except for quotations and summaries which have been duly acknowledged. The thesis has not been accepted for any degree and is not concurrently submitted for award of other degree.

Signature : ………………….

Name : NADIAH WAZNAH BINTI ZABIDI

ID Number : MA 05045

Date :

ACKNOWLEDGEMENTS

First I would like to express my grateful to Allah s.w.t. as for the blessing given that I can finish my project.

In preparing this thesis, I was contact with many people and academicians in helping me completing this project. They have contributed toward my understanding, and also guidance. First, I wish to express my sincere appreciation to my main thesis supervisor Mdm Mas Ayu Binti Hassan, for encouragement, valuable guidance, constructive criticism, advices, suggestion and motivation throughout this thesis. Without her continued support and interest, this thesis would not have been the same as presented here

My sincere also extends to all my beloved family especially my father Zabidi Bin Abd Rashid and my mother Siti Hasnah Bt Sheikh Mokhsin because of if not their prayer and support I would not be here and done this thesis. More over I would like to thanks for all my colleagues and others who provides assistance at various occasions. Their view and tips are useful indeed in helping me to achieve doing this thesis.

ABSTRACT

Wire electro discharge machining (WEDM) is a fully extended and competitive machining process widely used to produce dies and moulds. However, the risk of wire breakage affects adversely the full potential of WEDM since the overall process efficiency is considerably reduced. These symptoms are especially related to the occurrence of an increase in discharge energy, peak current, as well as increases or decreases in ignition delay time. Because of that, an experimental determination method of the convective heat transfer coefficient in wire electro discharge machining is introduced to prevent the wire breaks during running the machine. Parameters such as peak current and flushing pressure are studied. A special device is developed to measure the average temperature increment of the wire after a period of short circuit discharges, and the thermal load imposed on the wire is also tracked and recorded in advance. Then, based on the thermal model of the wire, the convective coefficient can be calculated accurately. Some tuning experiments are carried out inside and outside a previously cut profile to examine the influence of the kerf on the convective coefficient. With this method, the effect of the coolant flushing pressure on the convective coefficient can be estimated. Based on the results of the analyses, this paper contributes to improve the process performance through a wire breakage.

ABSTRAK

Mesin wayar nyahcas elektrik (WEDM) adalah mesin yang sangat kompetitif dan digunakan secara meluas dalam menghasilkan acuan. Walau bagaimanapun, risiko pemutusan wayar memberi kesan kepada potensi WEDM apabila keseluruhan kecekapan proses semakin berkurangan. Simptom ini berkaitan dengan kejadian peningkatan nyahcas tenaga, arus yang tinggi dan juga peningkatan serta pengurangan penangguhan masa nyalaan percikan elektrik. Oleh sebab itu, eksperimen kaedah penentuan pemalar peralihan haba secara perolakan dalam WEDM diperkenalkan bagi mengelakkan pemutusan wayar berlaku semasa mengendalikan mesin. Faktor pengehad seperti arus dan tekanan simbahan penyejuk juga dikaji. Purata kenaikan suhu wayar selepas nyahcas litar pintas dan beban haba yang dikenakan pada wayar dicatat. Kemudian berdasarkan model haba, pemalar perolakan haba dapat di tentukan dengan tepat. Beberapa eksperimen dijalankan untuk mengkaji kesan laluan pemotongan bahan ke atas pemalar peralihan haba secara perolakan. Tekanan simbahan penyejuk juga digunakan semasa eksperimen dan kesan tekanan simbahan ini ke atas pemalar peralihan haba secara perolakan juga dikaji.

TABLE OF CONTENTS

LIST OF TABLES

LIST OF FIGURES

LIST OF SYMBOLS

h	Convective heat transfer coefficient, W/ (m^{2}K)
x	Coordinate along wire axis, m
t	Time coordinate, s
T	Temperature increment along the wire at any time, K
ρ	Mass density, kg/m^3
c	Specific heat, J/(kg K)
Vw	Wire transporting speed, m/s
λ	Thermal conductivity of wire material, W/(m K)
av	Thermal diffusivity of wire material, m^2/s
L	Circumference of the wire, m
S	Cross section area of the wire, m^2
n	= hL/S
q'''	Heat flux density, W/m
q'''_J	Joule heat flux density, W/m
q'''_d	Discharge heat flux density, W/m
x_1, x_4	Coordinates of the current supplying positions
x_2, x_3	Coordinates of the top and bottom edge of the workpiece
ΔTa	Average temperature increment, K
r	Radius of the wire
$I_S(t)$	Value of the short circuit current, A

ts	Period of the discharging current pulse, s
$U_1(t)$	Output voltage of current sensor, V
R_1	Resistance of the series resistor, Ω
Ip	Peak current of the pulse, A
Q_1	Number of turns of the coil
α	Temperature coefficient of wire material, K^{-1}
U_O	Output voltage of the resistance measuring system, V
R	Resistance of the wire electrode between x_1 and x_4, Ω
Ic	Constant current, A
β	Amplification of the differential signal amplifier
ω	Cross section area of the wire, m^2

LIST OF ABBREVIATIONS

WEDM	Wire electro discharge machining
AISI	American iron steel institute

CHAPTER 1

INTRODUCTION

1.1 RESEARCH BACKGROUND

Wire electrical discharge machining (WEDM) is an adaptation of the basic EDM process, which can be used for cutting complex two and three dimensional shapes through electrically conducting materials. WEDM utilizes a thin, continuously moving wire as an electrode [10]. It is a relatively new process and applications have grown rapidly, particularly in the tool making field. The wire electrode is drawn from a supply reel and collected on a take up reel. This continuously delivers fresh wire to the work area. The wire is guided by sapphire or diamond guides and kept straight by high tension, which is important to avoid tapering of the cut surface [6]. High frequency dc pulses are delivered to the wire and workpiece, causing spark discharges in the narrow gap between the two. A stream of dielectric fluid is directed, usually coaxially with the wire, to flood the gap between the wire and the workpiece [7]. The power supplies for WEDM are essentially the same as for conventional EDM, except the current carrying capacity of the wire limits currents to less than 20A, with 10A or less being most normal. WEDM is most commonly used for the fabrication of press stamping dies, extrusion dies, powder composition dies, profile gages and templates [10].

1.2 PROBLEM STATEMENT

In WEDM process, the heat generated by continuous discharges will lead to the temperature increment and local erosion of the wire and consequently lower its tensile strength. Contradictorily, it is necessary to keep the wire tension at high level in order to guarantee the machining accuracy. To prevent the wire from breaking, the machining processes must take place in ionized water bath which not only aids in the sparking mechanism, but also helps cooling the wire. The accurately determined convective heat transfer coefficient will lead to exact analysis and hence will be helpful for the prediction of the wire breakage.

1.3 PROJECT OBJECTIVES

The objectives of this project :

i) To determine the convective heat transfer coefficient in WEDM.
ii) To discover the effect of the kerf on the convective coefficient.
iii) To investigate the effect of the flushing pressure on the convective coefficient.

1.4 PROJECT SCOPES

This project concentrates on determining the convective heat transfer coefficient in WEDM using brass wire material with diameter 0.2mm. The workpiece use in this project is AISI 4140 with diemension (200mm x 40mm x 15mm). The values of the convective coefficient change with the kerf conditions and in the presence of coolant flushing pressure.

CHAPTER 2

LITERATURE REVIEW

2.1 INTRODUCTION OF WEDM

Wire-electro discharge machining is a process of material removal of electrically conductive materials by the thermo-electric source of energy [3]. The material removal by controlled erosion through a series of repetitive sparks between electrodes, workpiece and tool. The electrode is a thin wire and it is pulled through the workpiece from a supply spool onto a take up mechanism [2,3]. On application of a proper voltage, discharge occurs between the wire electrode and the workpiece in the presence of a flood of deionized water of high insulation resistance[4]. WEDM using small diameter wires permits extremely narrow slots to be machined in the workpiece, and the kerf is only slighter wider than the wire diameter.

Figure 2.1 Wire Electro-Discharge Machining [4]

2.2 WEDM FUNCTION

WEDM has advanced quickly with the addition of computer numerical control (CNC). Today WEDM is used for a wide variety of precision metalworking applications which would have been almost impossible just a few years ago [8]. Cutting tolerances, cutting speeds and surface finish quality have been greatly improved [11]. Wire-cut EDM can do things older technologies cannot do as well, as quickly, as inexpensively, and as accurately. Most parts can now be programmed and produced as a solid, rather than in sections and then assembled as a unit that necessary. The WEDM is capable of producing complex shapes such as tapers, involutes, parabolas and ellipses that would otherwise be difficult to produce with conventional cutting tools [14,15].

2.3 WEDM OPERATING SYSTEM

Figure 2.2 below shows the basic operating of the WEDM machine. The WEDM move the workpiece along the X and Y axes (backward, forward, and sideways) in a horizontal plane toward a vertically moving wire . During the cutting action, an arc gap of 0.02mm to 0.05mm is maintained between the workpiece and the wire electrode [7]. The eroded material caused by the spark is then washed away by the dielectric fluid. The WEDM process, as shown in Figure 2.2 also generates the desired shape by using electrical sparks between a thin, traveling brass wire electrode and workpiece to erode a path in the workpiece material [6,7]. It also shows continuous electrical sparks being generated between the wire and workpiece for material removal. The cutting force generated in WEDM is small, which makes it suitable for manufacturing miniature features and micro-mechanical components [7].

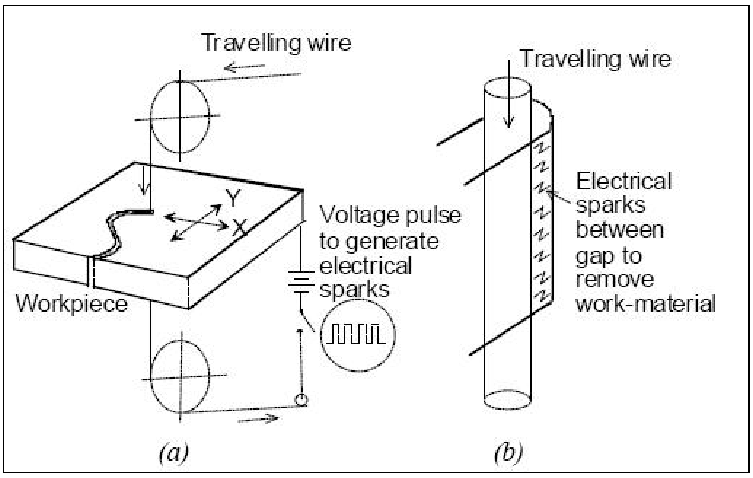

Figure 2.2 Conventional 2D WEDM operation [2]

2.3.1 Operation Panel

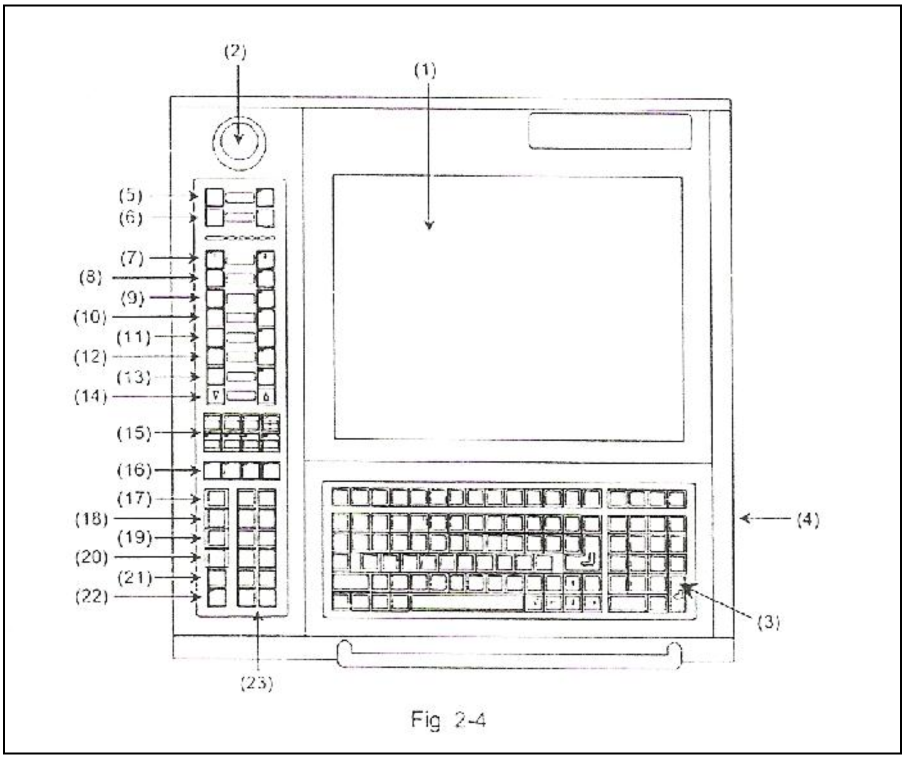

Figure 2.3 Operation panel of WEDM [2]

(1)	LCD screen	(13)	[TANKDRAIN ON/OFF]
(2)	Emergency stop switch	(14)	[TANK DOOR]
(3)	Keyboard	(15)	Switches [A0] to [A7]
(4)	Floppy disc drive	(16)	[MFR0] to [MFR3]
(5)	[SOURCE ON/OFF] switches	(17)	[OFF] switch
(6)	[POWER ON/OFF] switches	(18)	[ACK] switch
(7)	[AWT CUT/TREAD] switch	(19)	[HALT] switch
(8)	[TENSION ON/OFF] switches	(20)	[ENT] switch
(9)	[WIRE STOP/RUN] switches	(21)	[ST] switch
(10)	[HIGH PRESSURE ON/OFF] switches	(22)	[UV] switch
(11)	[LOW PRESSURE ON/OFF] switches	(23)	Jog switches
(12)	[TANK FILL ON/OFF]		

2.3.2 Dielectric Fluid

One of the most important factors in a successful WEDM operation is the removal of the particles (chips) from the working gap. Flushing these particles out of the gap with the dielectric fluid will produce good cutting conditions, while poor flushing will cause erratic cutting and poor machining conditions [10].

The dielectric fluid in the WEDM process is usually deionized water. This is tap water that is circulated through an ion-exchange resin. The deionized water makes a good insulator, while untreated water is a conductor and is not suitable for the electrical discharge machining process[11,13]. The amount of deionization of the water determines its resistance. For most operations, the lower the resistance the faster will be the cutting speed [10].

The dielectric fluid used in the WEDM process serves several functions :

1. It helps to initiate the spark between the wire and the workpiece [2].
2. It serves as an insulator between the wire and the workpiece [2].
3. It flushes away the particles of disintegrated wire and workpiece to prevent shorting [3].
4. It acts as a coolant for both the wire and the workpiece [3].

2.4 MILLING MACHINE

A milling machine is a machine tool used for the shaping of metal and other solid materials. Its basic form is that of a rotating cutter which rotates about the spindle axis (similar to a drill), and a table to which the workpiece is affixed. In contrast to drilling, where the drill is moved exclusively along its axis, the milling operation involves movement of the rotating cutter sideways as well as in and out [14].

The cutter and workpiece move relative to each other, generating a tool path along which material is removed. The movement is precisely controlled, usually with slides and lead screws or analogous technology [13]. Often the movement is achieved by moving the table while the cutter rotates in one place, but regardless of how the parts of the machine slide, the result that matters is the relative motion between cutter and workpiece. Milling machines may be manually operated, mechanically automated, or digitally automated via CNC [14].

Milling machines can perform a vast number of operations, some of them with quite complex tool paths, such as slot cutting, planing, drilling, diesinking, rebating and routing. Cutting fluid is often pumped to the cutting site to cool and lubricate the cut, and to sluice away the resulting swarf.[14].

Figure 2.4 Milling machine [14]

Most CNC milling machines or machining centers are computer controlled vertical mills with the ability to move the spindle vertically along the Z-axis. This extra degree of freedom permits their use in die sinking, engraving applications, and 2D surfaces such as relief sculptures [13]. When combined with the use of conical tools or a ball nose cutter, it also significantly improves milling precision without impacting speed, providing a cost-efficient alternative to most flat-surface hand-engraving work [11].

CNC machines can exist in virtually any of the forms of manual machinery, like horizontal mills. The most advanced CNC milling-machines, the 5-axis machines, add two more axes in addition to the three normal axes (XYZ). Horizontal milling machines also have a C or Q axis, allowing the horizontally mounted workpiece to be rotated, essentially allowing asymmetric and eccentric turning [13]

2.5 MATERIALS

2.5.1 Wire Materials

The wire material used in this project is made of brass, which is an ideal material for the thermal resistance. It is an alloy of copper and zinc that has good corrosion resistance and is easily formed, machined and cast [9]. Copper is the main component, and brass is usually classified as a copper alloy. The color of brass varies from a dark reddish brown to a light silvery yellow depending on the amount of zinc present. The more zinc, the lighter the color. Brass is stronger and harder than copper, but not as strong or hard as steel [6]. It is easy to form into various shapes, a good conductor of heat, and generally resistant to corrosion from salt water. Because of these properties, brass is used to make pipes and tubes, weather-stripping and other architectural trim pieces, screws, radiators, musical instruments, and cartridge casings for firearms [9]. It has consistent tensile strength which is the heat treated for stable tensile strength to avoid the wire breakage [1].

Figure 2.5 Brass material [3]

2.5.2 Mechanical Properties of Brass Wire

Table 2.1 : Compositon of Brass [12]

Component	Wt.%
C	60 - 63
Zn	35.5
Pb	2.5 - 3.7
Fe	Max 0.35
Other	Max 0.5

Brass consists of five elements which copper has the highest percentage of the composition. The percentage is between 60 to 63 percent and it follows by zinc. The percentage of zinc element in brass is 35.5 percent and follows by lead 2.5 to 3.7 percent, iron 0.35 percent and other element is 0.5 percent [12].

Table 2.2 : Mechanical Properties of Brass [12]

Mechanical Properties	Metric
Ultimate Tensile Strength	338 – 469 Mpa
Tensile Strength, Yield	124 – 310 Mpa
Elongation at Break	53%
Modulus of Elasticity	97 Gpa
Bulk Modulus	140 Gpa
Poisson's Ratio	0.31
Machinability	100%
Shear Modulus	37 Gpa

Table 2.2 shows mechanical properties of brass. Brass has Ultimate Tensile Strength between 338 to 469 Mpa and Tensile Strength , Yield varies from 124 to 310 Mpa. The elongation at break is 53%, Modulus of Elasticity 97 Gpa and Bulk Modulus is 140 Gpa. The Poisson's Ratio of brass is 0.31, Shear Modulus 37 Gpa and it has 100% machinability [12].

2.5.3 Workpiece Material

The workpiece material used is AISI 4140. This steel is choose because it is suitable for heavy duty service due to high hardenability, good abrasion, high wear resistance, strength and durability [9]. AISI 4140 plate is used especially in the automotive industry for tool and die, as die plates, injections molds as mold plates, and for machine bases and blocks. AISI 4140 Steel also known as chromium molybdenum alloy steel is oil hardening steel of relatively high hardening ability and is among the most widely used versatile machinery steels [10]. The chromium content provides good hardness penetration and the molybdenum imparts uniformity of hardness and high strength. This grade is especially suitable for forging as it has self scaling characteristics it responds readily to heat treatment and is comparatively easy to machine in the heat treated condition. In the heat treated condition tensile strengths are attended all combined with good ductility and resistance to shock. This steel maintains its properties even after long exposure at these relatively high working temperatures [6].

Table 2.3 : Composition of AISI 4140 steel [10]

Element	Weight %
C	0.38-0.43
Mn	0.75-1.00
P	0.035
S	0.04
Si	0.15-0.30
Cr	0.80-1.10
Mo	0.15-0.25

The composition of AISI 4140 Steel used in this project is presented in Table 2.3. The composition including Copper 0.38 to 0.43 percent, Manganese 0.75 to 1.00 percent, Sulfur 0.04 percent and the least is Phosphorus 0.035 percent. In the composition of AISI 4140 Steel, Chromium has the highest percentage which is from 0.8 to 1.10 percent while Silicon 0.15 to 0.30 percent and lastly Molybdenum 0.15 to 0.25 percent.

2.5.4 Temperature distribution for brass wire material

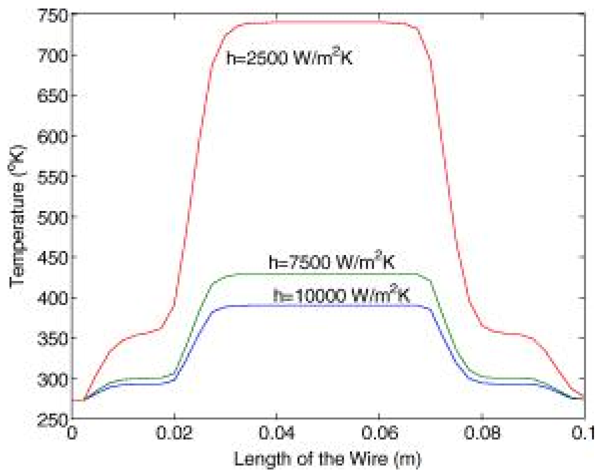

Figure 2.6 Graph temperature distribution for brass wire material [9]

Figure 2.6 shows the temperature distribution along the length of the wire. The temperature of the wire increase when the convective heat transfer coefficient decrease. The baseline temperature is 273K and it continues increase to 380K when the value of h is 10 000 W/ m^2 K.

2.6 CONVECTIVE HEAT TRANSFER

Convection is the mode of energy transfer between a solid surface and the adjacent liquid or gas that is in motion, and it involves the combined effects of conduction and fluid motion. The faster the fluid motion, the greater the convective heat transfer [4]. Consider two regions separated by a barrier as shown in Figure 2.7. One at a higher pressure while the other at a lower pressure. Then the barrier was removed as in the following figure. These convection currents are illustrated in the figure below

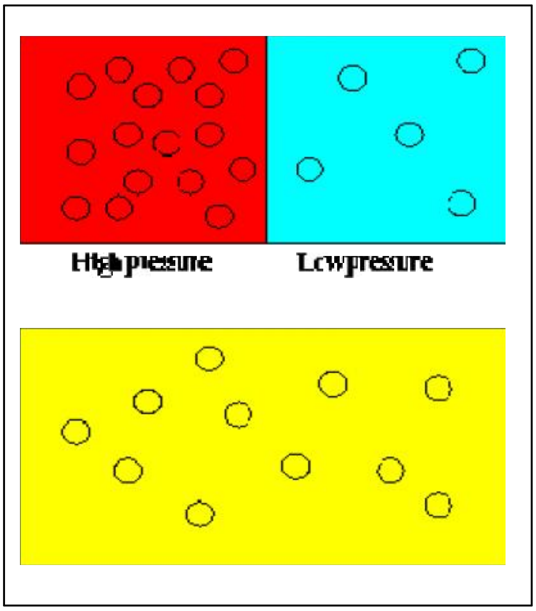

Figure 2.7 Flow of material through a pressure difference [4]

When the barrier is removed, material in the high pressure (high density) area will flow to the low pressure (low density) area. If the low pressure region was originally created by heating of the material, one sees that movement of material in this way is an example of heat flow by convection [4].

Convective heat transfer may take the form of either [4]:

i) Forced convection ii) Free convection

2.6.4 Forced Convection

Convection is called forced convection if the fluid is forced to flow over the surface by external means such as fan, pump, or the wind [4].

2.6.5 Free Convection

Convection is called free convection if the fluid motion is caused by buoyancy forces that are induced by density differences due to the variation of temperature in the fluid [4] .

2.6.3 Convective Heat Transfer Coefficient

The convection heat transfer coefficient h is not a property of the fluid. It is an experimentally determined parameter whose value depends on all the variables influencing convection such as the surface geometry, the nature of fluid motion, the properties of fluid and the bulk fluid velocity [1]. Typical values of h are given in Table 2.4

Table 2.4 : Typical values of convection heat transfer coefficient

Type of convection	h, $W/m^2.^0C$
Free convection of liquids	10 - 1000
Free convection of gases	2 - 25
Forced convection of liquids	50 - 20000
Forced convection of gases	25 - 250
Boiling and condensation	2500 - 100000

In WEDM process, the heat generated by continuous discharges will lead to the temperature increment and local erosion of the wire, and consequently lower its tensile strength. Contradictorily, it is necessary to keep the wire tension at a high level in order to guarantee the machining accuracy. So wire breakage is inevitable if heat generated by continuous discharge cannot be taken away effectively and timely.

It is a critical problem for the development of the WEDM method especially for the micro-WEDM where the micro-wire is easier to break than ordinary wire. To prevent the wire from breaking, the machining processes must take place in an ionized water bath, which not only aids in the sparking mechanism, but also helps cooling the wire when the water flushes along the wire. Such convective cooling has a major influence on the removal of discharging heat away from the discharging zone. The cooling efficiency can be quantified by the convective heat transfer coefficient of the coolant, which is a critical variable used to define the amount and ratio of the heat convected away from the wire. Moreover, the convective heat transfer coefficient is one of the most important parameters for analyzing the temperature distribution and crater formation of the wire[1,2]. The accurately determined convective coefficient will lead to exact analysis, and hence will be helpful for the prediction of the wire breakage.

Unfortunately, it is not easy to measure or calculate this coefficient directly, and even an order of magnitude estimation is considered to be difficult. In the literature [3], the values of the convective heat transfer coefficient *h* cover a very wide range for forced convection in liquids: h=50–20,000 W/m^2 K. In case of convection with phase change (boiling or condensation), an even larger range is indicated (h=2500–1,00,000 W/m^2 K). The above values ranges so wide that they are of little significance in the actual heat transfer analysis.

According to Tanimura and Kinoshita they had estimated the convective heat transfer coefficient by evaluating the time constants associated with the cooling rate of the wire. Considering that the measurement of such time constants is difficult itself, this method also has its limitation for its lack of accuracy [4,5].

Jennes experimentally determined the convective heat transfer coefficient by imposing a known thermal load on the wire in and outside a previously cut profile. Simultaneously, mechanical stresses were applied approximating those associated with normal cutting conditions [6]. Using the temperature dependency of the mechanical strength of the wire material, a rough estimation of the heat transfer coefficient was found as shown in Table 2.5 .Satoshi proposed a method to measure the wire temperature by utilizing the relationship between the wire temperature and the sensitivity change of the method of measuring discharge location [7].

Then in the Masanori's literature based on the differential equation for heat flow in the wire electrode, the convective coefficient was derived with the measured temperature [8]. Up to now however, the measurement of discharge locations is not accurate enough to a usable level, so that the measured temperature by Satoshi cannot provide a satisfied estimation of the convective coefficient in WEDM process [7] .

Table 2.5 : Rough estimation of the convective coefficient [7]

Workpiece thickness (mm)	**Outside workpiece (W/m^2K)**	**Inside workpiece (W/m^2K)**
10	15500	15700
50	12800	6800

Obviously, it is the lack of accuracy that limits the above methods to be widely used in the determination of convective coefficient in WEDM process. To get a more accurate estimation of the convective heat transfer coefficient, an experimental determination method is introduced in this project .

With this method, the value of convective coefficient under different flushing pressure of the coolant is determined. Some additional experiments were also carried out in and outside a previously cut profile to examine the influence of the kerf on the convective coefficient.

2.7 KERF

Kerf is a slit or width of cut made by a saw or cutting torch. The brass wire will carried out inside and outside a previously cut profile to examine the influence of the kerf on the convective coefficient. The values of the convective coefficient change with the kerf conditions. As soon as the wire cuts into the workpiece, the convective coefficient will decrease more than 30%. [3]

The table below shows whatever value the Ip is set the experimentally determined value of h keeps approximately the same as long as the flushing pressure and the kerf condition are fixed. According to the table, it can be seen that the coefficient h is much larger outside of the kerf than inside of the kerf.

Table 2.6 : The effect of kerf on the convective coefficient h

Kerf condition	Convective coefficient h (W/m^2K)		
	Ip = 254A	Ip = 332A	Ip = 414A
Inside kerf	17626.0	17385.3	18234.7
Outside kerf	23507.5	24101.5	23889.7

2.8 COOLANT FLUSHING PRESSURE

It is important to prevent the wire from overheat by flushing the coolant toward the wire. The coolant helps cooling the wire when the water flushes along the wire. Increased flushing pressure of the coolant can lower the average temperature increment of the wire during the WEDM process [1]. The larger the flushing pressure is, the larger the coefficient h will be. Table 2.7 showed the effect of flushing pressure on the value of h. If the pressure is raised from 0.1 to 0.8 Mpa, the convective coefficient will increase about 30% when the wire is inside the kerf and about 23% when the wire is outside the kerf [1]. Whether the wire is inside the kerf or not, the convective coefficient will increase with the increased flushing pressure of the coolant and thus the cooling condition of the WEDM process is ameliorated [1,3].

Table 2.7 : The effect of flushing pressure on the convective coefficient h [1]

Kerf condition	Convective coefficient h (W/m^2K)	
	Pressure = 0.1 Mpa	Pressure = 0.8 Mpa
Inside kerf	17626.0	17385.3
Outside kerf	23507.5	24101.5

CHAPTER 3

METHODOLOGY

3.1 INTRODUCTION

This chapter presents a details discussion about the methodology structures of this study. The chapter begins with general overview of the methodology adopted, followed by experiments. In this project there are two machines used which are milling machine and WEDM. The workpiece was cut into the desired shape and accurate dimension using milling machine. Then the workpiece was cut into 9 small portion by using WEDM. Input data such as different peak current, flushing pressure, wire speed and wire tension were inserted to the machine screen. After the experiment finished, all the output data were taken and the calculation of temperature increment for each peak current by using formula was done. This is followed by analysis of the result which is graph were created to analyze the results obtained.

Once the results were analyzed, the discussion of the experiment must be determined. Lastly, the conclusion must be done to conclude all the result and discussion as well. If there is any recommendations or adjustment regarding the experiments, then it has to be clearly stated in order to make further experiments run more effective.

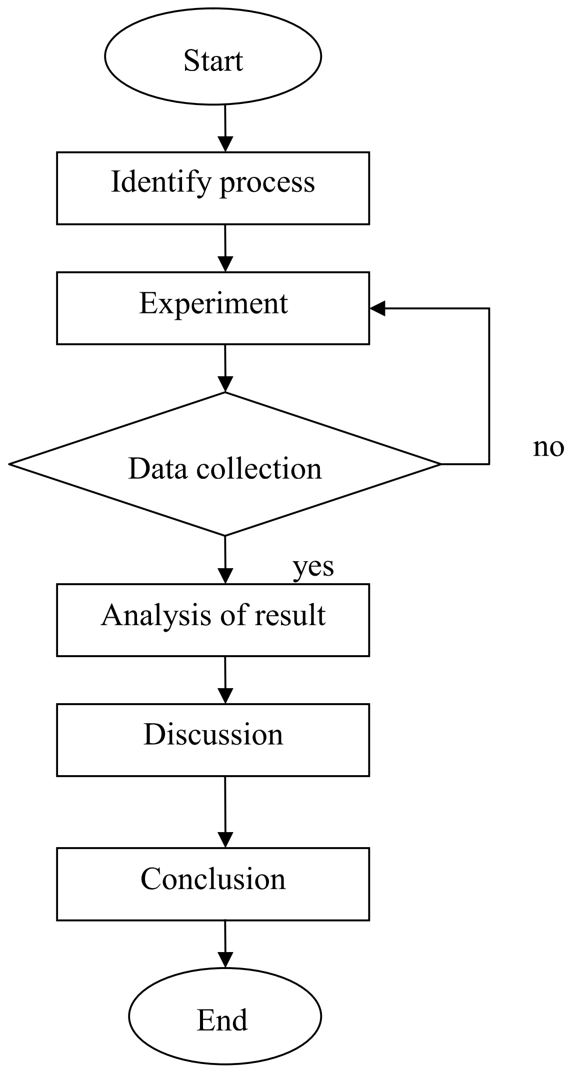

Figure 3.1 Flowchart outlining the steps taken in this project

3.1.1 Experiment Flowchart

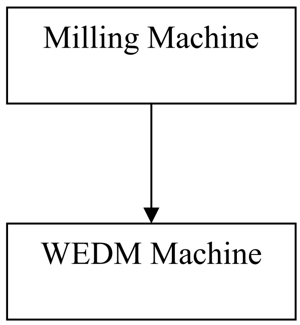

Figure 3.2 Flowchart of experiment

Before the workpiece was cut into 9 portion , the corrosion of the workpiece must be removed. The milling machine was used to make sure the workpiece is cut into desired shape and dimension. Then after the process, the workpiece can be cut using WEDM machine. Some of the precaution steps should be taken before running the WEDM machine. There must be a gap which is 0.1mm between the wire and the workpiece . If there is no gap, short circuit current will occur and wire will break. Besides that, air pressure must be sufficient during operating the experiment.

3.2 IDENTIFY PROCESS

During the WEDM process, there are two types of heating energy are inputted into the wire. There are Joule heating energy and the discharging energy. Joule heating energy is generated by the short circuit current while the discharging energy is generated by normal discharges between the wire and the workpiece. The discharging energy is simplified as evenly distributed in the wire body considering that the discharges occur at high frequency.[1]

In this manner, the effect of discharges is thus represented by a uniform time invariant q'''_d which means the amount of energy generated by discharges per unit volume and per unit time [2]. Joule heating energy is represented by using another uniform time invariant q'''_J . The wire lose part of its thermal energy by the effect of convection and conductions as it is immersed in an infinite fluid medium with a uniform temperature at infinity. Based on the above assumptions, Tanimura [4] had established a simplified thermal model for the WEDM process in Figure 3.3

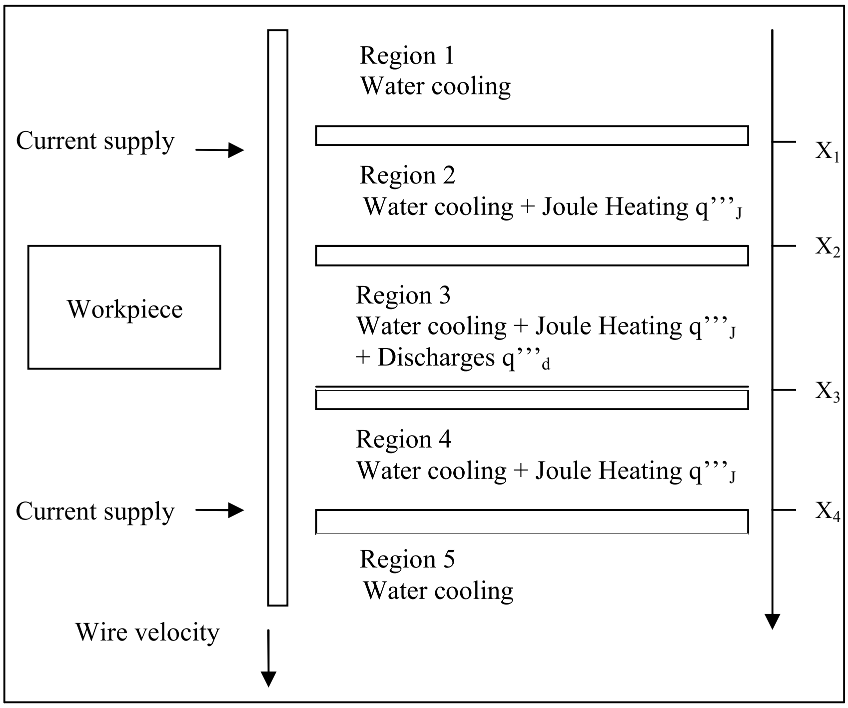

Figure 3.3 Thermal model for the WEDM process [4]

Figure 3.3 shows a thermal model for the WEDM process which shows. During a typical electro discharge machining process, considering the wire is traveling in the direction of *x* axis, any part of the wire will pass through 5 regions separated by the position of x_1–x_4. In region 3, consecutive electro discharges and Joule energy heat up the wire body, which is also cooled at the same time by the coolant. In regions 2 and 4, the wire locates outside the kerf, so there is no discharge energy applied on the wire, but only Joule heating energy. In regions 1 and 5, there is neither short circuit current nor electro discharges acted on the wire, but only cooling effect [4]

According to thermal load , a 1-D differential equation for heat flow in an infinite body , moving with a constant velocity V_w can be written as

$$\frac{\partial^2 T(x,t)}{\partial x^2}-\frac{\rho c V_w}{\lambda}\frac{\partial T(x,t)}{\partial x}=\frac{1}{a}\frac{\partial T(x,t)}{\partial t}+\frac{hL}{S\lambda}T(x,t)-\frac{q'''}{\lambda}, \qquad (1)$$

Theoritically , the temperature increment T (x,t) along the wire can be calculated at anytime using the above equation. If the wire is in the static condition that is $V_w = 0$ and q''' is constant , then in the case of a stationary state , the differential equation of heat flow has the following form :

$$\frac{d^2T}{dx^2}-\frac{n}{\lambda}\cdot T+\frac{1}{\lambda}\cdot q'''=0 \qquad (2)$$

With n = hL/S

The discharging current is supplied to the wire only from one point at the position of x_1. At the position of x_4, the wire is connected to the cathode of the pulse generator. In order to avoid the normal discharges being generated between the wire and the workpiece, the workpiece is insulated from the wire at the same time. So only short circuit current pulses will flow through the part of the wire from x_1 to x_4. Only the Joule heating energy and the mean value of which is a constant is supplied to that part of the wire.

The temperature increment of the wire in region 1 is stated as T_1 , in regions 2, 3, 4 as T_2 and in region 5 as $T_{3,}$ thus the differential equation (2) becomes the following differential equations :

$$\begin{cases} \frac{d^2 T_1}{dx^2} - nT_1 = 0, & x \in (-\infty, x_1) \\ \frac{d^2 T_2}{dx^2} - nT_2 + \frac{1}{\lambda} q'''_J = 0, & x \in [x_1, x_4] \\ \frac{d^2 T_3}{dx^2} - nT_3 = 0, & x \in (x_4, +\infty) \end{cases} \tag{3}$$

with the boundary conditions

$$\begin{aligned} &T_1\big|_{x=-\infty} = 0, && \frac{dT_1}{dx}\Big|_{x=-\infty} = 0, \\ &T_1(x_1) = T_2(x_1), && \frac{dT_1}{dx}\Big|_{x=x_1} = \frac{dT_2}{dx}\Big|_{x=x_1}, \\ &T_2(x_4) = T_3(x_4), && \frac{dT_2}{dx}\Big|_{x=x_4} = \frac{dT_3}{dx}\Big|_{x=x_4}, \\ &T_3\big|_{x=+\infty} = 0, && \frac{dT_3}{dx}\Big|_{x=+\infty} = 0, \end{aligned}$$

which means the temperature distribution along the wire is continuous and smooth with a uniform temperature at infinity. By solving equation (3) with the above boundary conditions, the temperature distribution of the wire between x_1 and x_4 can be expressed as

$$T_2(x) = \frac{q'''_J}{n\lambda}\left[1 - \frac{1}{2}\exp\sqrt{n}(x - x_4) + \frac{1}{2}\exp\sqrt{n}(x_1 - x)\right]. \tag{4}$$

Then the average temperature increment of the wire between x_1 and x_4 caused by the Joule heat will be

$$\Delta T_a = \frac{\int_{x_1}^{x_4} T_2(x)dx}{x_4 - x_1} = \frac{q'''_J}{n}\left[1 - \frac{1 - \exp(-m)}{m}\right], \tag{5}$$

Where $m = \sqrt{n/\lambda}(x_4 - x_1) = \sqrt{\left(2h \cdot (x_4 - x_1)^2 / (\lambda \cdot r)\right)}$

If the part of the wire between x_1 and x_4 is long enough compared with the wire radius that is $(x_4 - x_1) > r$, then equation (5) can be simplified as

$$\Delta T_a = \frac{q'''_J}{n} = \frac{S}{L \cdot h} q'''_J = \frac{r}{2h} q'''_J . \tag{6}$$

Then h can be determined as

$$h = \frac{1}{2} \cdot \frac{r \cdot q'''_J}{\Delta T_a} . \tag{7}$$

Now that q'''_J and ΔT_a are necessary variables for the determination of the convective heat transfer coefficient, experimental determination of them should be accomplished first.

3.3 EXPERIMENT

3.3.1 Experimental Determination of the Joule heat flux

Joule heat flux density that loaded on the wire can be defined as

$$\begin{aligned} q'''_J &= \frac{1}{t_S S(x_4 - x_1)} \cdot \int_0^{t_S} I_S(t)^2 R \mathrm{d}t \\ &= \frac{R}{\pi t_S r^2 (x_4 - x_1)} \cdot \int_0^{t_S} I_S(t)^2 \mathrm{d}t \\ &= A \cdot \frac{R}{\pi r^2 (x_4 - x_1)} \end{aligned} \tag{8}$$

with

$$A = \int_0^{t_S} I_S(t)^2 \mathrm{d}t \Big/ t_S , \tag{9}$$

When the short circuit current pulses flow through the wire, induced electrical current is generated in the coil of the sensor, which can be easily converted into a voltage signal $U_1(t)$ by a resistor of 1.2 Ω connected in series

$$\mathbf{Is(t) = \{U_1(t) / R_1\}Q_1} \tag{10}$$

Table 3.1 : Short circuit current with different peak current

Ip (A)	200	300	400
Short circuit current			

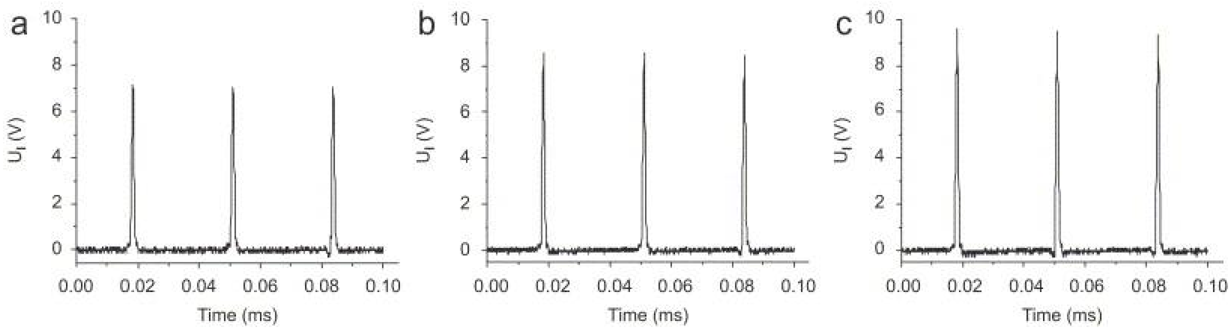

Figure 3.4 $U_1(t)$ with different Ip setting [1]

The experiment includes different peak currents which are 200A, 300A and 400A. Then based on the graph that has been captured and recorded, the value of $U_1(t)$ can be known. The larger the Ip is, the higher can the $U_1(t)$ reaches. The value of A then can be calculated when the value of $U_1(t)$ is insert in equation no 9. As soon as A is known, the Joule heat flux density that loaded on the wire can be determined by using equation 8. The value of A represents how much Joule heat flux density has been loaded on the wire electrode.

3.3.2 Experimental System for Determining the Average Temperature Increment of the Wire

The Δ Ta of the wire can be determined by using the relationship between the Δ Ta of the wire and U_o

$$\Delta T_a = \frac{\Delta R_t}{R_t} \cdot \frac{1}{\alpha} = \frac{U_o - U_{o0}}{U_{o0}} \cdot \frac{1}{\alpha}, \tag{11}$$

When combining equations (7) , (8) and (11), the convective heat transfer coefficient can be simplified as

$$h = \frac{1}{2} \cdot \frac{r \cdot q'''_J}{\Delta T_a} = \frac{A\alpha R}{2\pi r(x_4 - x_1)(U_0 - U_{o0})}. \tag{12}$$

Because of the electrical current that flows through the wire is a constant as shown in Figure 3 , the value of R can be determined. The relationship between the output voltage and *R* can be expressed as

$$R = U_o/(I_c \cdot \beta), \tag{13}$$

The resistance of the wire has a direct ratio with its length as well as with the output voltage of the resistance measuring system. So the length of the wire electrode between x_1 and x_4 has a direct ratio with U_o, and can be expressed as

$$x_4 - x_1 = U_o/\omega, \tag{14}$$

Then combined equations (12), (13) and (14) and it the final equation that is used to determine the convective heat transfer coefficient for the WEDM process can be simplified as

$$h = A\alpha\omega U_0 / 2\pi r\beta\ (U_0 - U_{o0}) \tag{15}$$

3.4 Data Collection

The Taguchi's Robust Design was used to determine the number of experiment that can be done during the operation. Four levels of each factor were chosen, table 3.2 shows the selected levels for the WEDM factors.

Specimen was cut with dimension 200mm x 40mm x 15mm from a rectangular bar of AISI 4140 steel. Specimen was cut using wire electro discharge machining cutting process. Table 3.3 shows the machining condition (on-time duration, peak current setting and flushing pressure) for the 16 experiments.

Table 3.2 : Factor levels for WEDM

Level	On-time duration (μs)	Peak current (A)	Flushing pressure (Mpa)
1	750	100	0.3
2	500	200	0.6
3	250	300	0.9
4	120	400	1.2

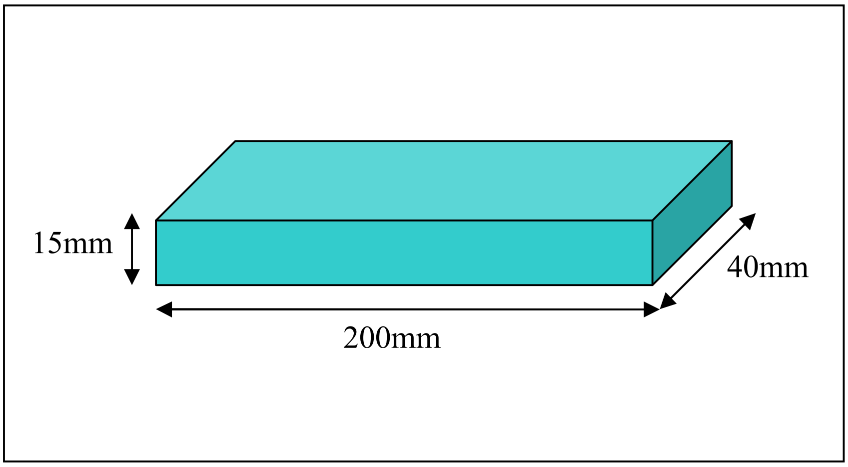

Figure 3.5 Specimen with dimension 200mm x 40mm x 15mm

Table 3.3: Input and Output Data

	Input data			**Output data**		
Number	**On-time duration (μs)**	**Peak current (A)**	**Flushing pressure (mm/s)**	**Voltage reading (V)**	**Temperature increment (K)**	**Machining time**
1	750	100	0.3			
2	750	200	0.6			
3	750	300	0.9			
4	750	400	1.2			
5	500	100	0.3			
6	500	200	0.6			
7	500	300	0.9			
8	500	400	1.2			
9	250	100	0.3			
10	250	200	0.6			
11	250	300	0.9			
12	250	400	1.2			
13	120	100	0.3			
14	120	200	0.6			
15	120	300	0.9			
16	120	400	1.2			

CHAPTER 4

RESULT AND DISCUSSION

4.1 OUTPUT VOLTAGE

Firstly, the temperature measurement experiments were carried out under the condition of different Joule heating energy input which can be adjusted in accordance with the peak current flowing through the wire. For each value of I_p, the average temperature increment of the wire was measured respectively when the wire was both inside and outside the kerf. Table 4.1 below shows the value of output voltage for both of the inside and outside kerf conditions. The current was set from 200A to 300A and it reaches to 400A. Then after the output voltage is known, the temperature increment ΔTa of the wire can be calculated by using equation 15

Table 4.1 : Output voltage of temperature measurement system for Ip = 200A

Time (ųs)	Output Voltage (V)	
	Inside kerf	Outside kerf
1.2×10^{-3}	1.90	1.83
1.5×10^{-3}	1.80	1.63
1.8×10^{-3}	1.78	1.57
2.1×10^{-3}	1.76	1.50

Table 4.1 above shows the result of output voltage for peak current 200A The output voltage of the wire is decreasing either the wire is hidden inside kerf or the outside kerf. When the wire is inside kerf, the value is decreasing from 1.9V to 1.76V and from 1.83V to 1.5V when the wire is outside kerf. Although both of the voltage is decreasing, the voltage inside kerf is higher rather than the outside kerf.

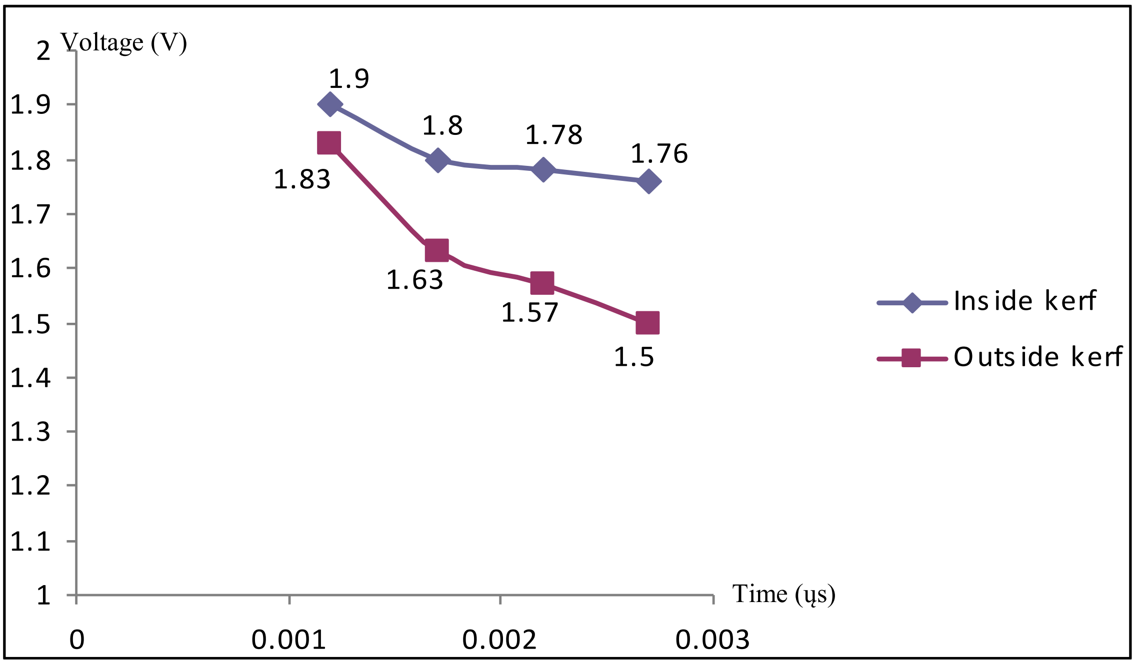

Figure 4.1 : Graph of voltage vs time for peak current 200A

Table 4.2 : Output voltage of temperature measurement system for Ip = 300A

Time (ųs)	Output Voltage (V)	
	Inside kerf	Outside kerf
1.2×10^{-3}	1.76	1.67
1.5×10^{-3}	1.72	1.55
1.8×10^{-3}	1.68	1.48
2.1×10^{-3}	1.66	1.45

Table 4.2 above shows result of output voltage for peak current 300A. At 1.2×10^{-3} ųs, the voltage inside kerf is 1.76V and the voltage outside kerf is 1.67V. The values are decreasing for both of the conditions and the voltage inside kerf is still higher compare to voltage outside kerf

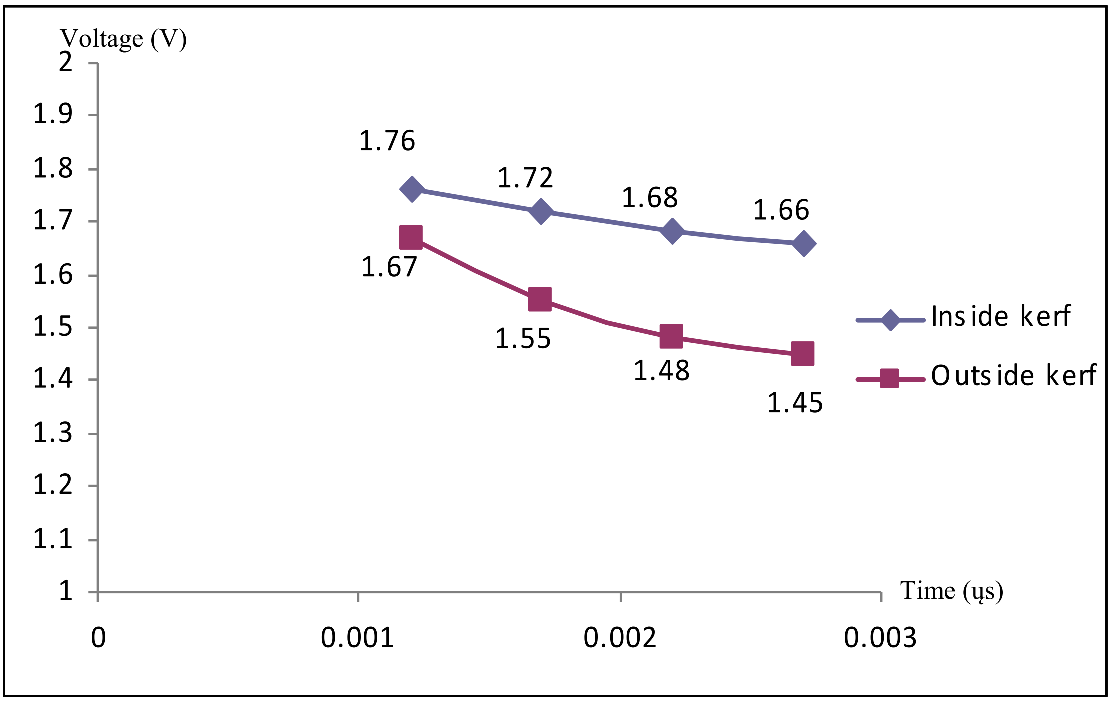

Figure 4.2 : Graph of voltage vs time for peak current 300A

Table 4.3 : Output voltage of temperature measurement system for Ip = 400A

Time (ųs)	Output Voltage (V)	
	Inside kerf	Outside kerf
1.2×10^{-3}	1.73	1.70
1.5×10^{-3}	1.66	1.57
1.8×10^{-3}	1.65	1.55
2.1×10^{-3}	1.64	1.54

Table 4.3 above shows the result of output voltage for peak current 400A. The output voltage inside kerf remains higher than the outside kerf when the current is set at 400A. At 1.2×10^{-3} ųs, voltage inside kerf is 1.73V and voltage outside kerf is 1.70V. The voltage for both conditions is decrease as time increase.

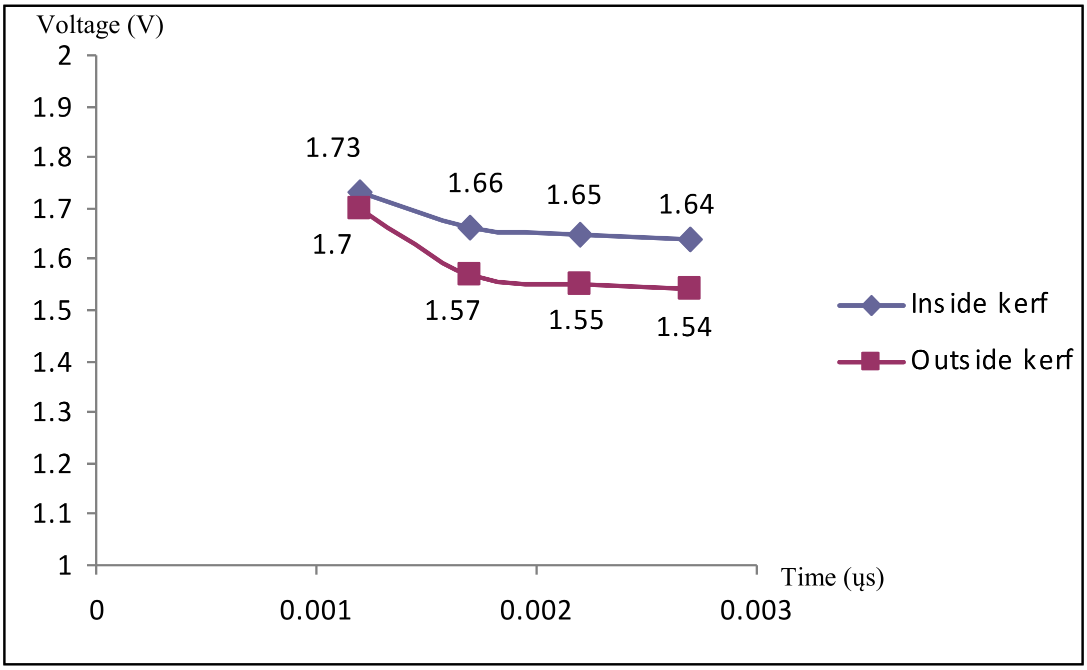

Figure 4.3 : Graph of voltage vs time for peak current 400A

4.2 TEMPERATURE INCREMENT

After the output voltage of each peak current and kerf conditions is known, then the temperature increment can be calculated by using equation 15. The experiments were conduct with the presence of flushing pressure which are 0.8Mpa and 0.1Mpa. The results of the temperature are different for both of the flushing pressure.

Table 4.4 : Temperature measurement with different peak current value and kerf conditions (Flushing pressure = 0.8 Mpa)

Kerf conditions	Temperature increment (K)		
	Ip = 200A	Ip = 300A	Ip = 400A
Inside kerf	268	269	271
Outside kerf	261	264	267

Table 4.4 shows the temperature increment of the wire with the presence of flushing pressure 0.8Mpa. The temperature increment of the wire rises considerably when the wire is hidden inside kerf .The temperature of the wire is increase from 268K to 271K inside kerf, and from 261K to 267K outside kerf. The results are obtained from the calculation shown below.

$\Delta Ta = (Uo - Uo0) / Uo0\ \alpha \quad \alpha = 0.01540$

Peak current 200A

$$\begin{aligned}\Delta Ta_{\text{inside kerf}} &= (1.76 - 1.90) / (1.90 \text{ x } 0.01540) \\ &= -4.785\ ^{o}C \\ &= -4.785 + 273K \\ &= 268K\end{aligned}$$

$$\begin{aligned}\Delta Ta_{\text{outside kerf}} &= (1.50 - 1.83) / (1.83 \text{ x } 0.01540) \\ &= -11.710\ ^{o}C \\ &= -11.710 + 273K \\ &= 261K\end{aligned}$$

Peak current 300A

$$\begin{aligned}\Delta Ta_{\text{inside kerf}} &= (1.66 - 1.76) / (1.76 \text{ x } 0.01540)\\ &= -\ 3.689\ ^{0}C\\ &= -\ 3.689 + 273 \text{ K}\\ &= 269 \text{ K}\end{aligned}$$

$$\begin{aligned}\Delta Ta_{\text{outside kerf}} &= (1.45 - 1.67) / (1.67 \text{ x } 0.01540)\\ &= -\ 8.554\ ^{o}C\\ &= -\ 8.554 + 273K\\ &= 264K\end{aligned}$$

Peak current 400A

$$\begin{aligned}\Delta Ta_{\text{inside kerf}} &= (1.64 - 1.73) / (1.73 \text{ x } 0.01540)\\ &= -\ 2.252\ ^{o}C\\ &= -\ 2.252 + 273K\\ &= 271K\end{aligned}$$

$$\begin{aligned}\Delta Ta_{\text{outside kerf}} &= (1.54 - 1.70) / (1.70 \text{ x } 0.01540)\\ &= -\ 6.112\ ^{o}C\\ &= -\ 6.112 + 273K\\ &= 267K\end{aligned}$$

Table 4.5 : Temperature measurement with different peak current value and kerf conditions (Flushing pressure =0.1Mpa)

Kerf conditions	Temperature increment (K)		
	Ip = 200A	Ip = 300A	Ip = 400A
Inside kerf	271	280	284
Outside kerf	267	270	273

Table 4.5 shows the temperature increment of the wire with the presence of flushing pressure 0.1Mpa. During peak current reaches to 400A, the temperature increment is 284K when the wire is inside kerf and 273K when the wire is outside kerf. Temperature increment increase as the peak current increase.

4.3 TEMPERATURE WITH DIFFERENT FLUSHING PRESSURE

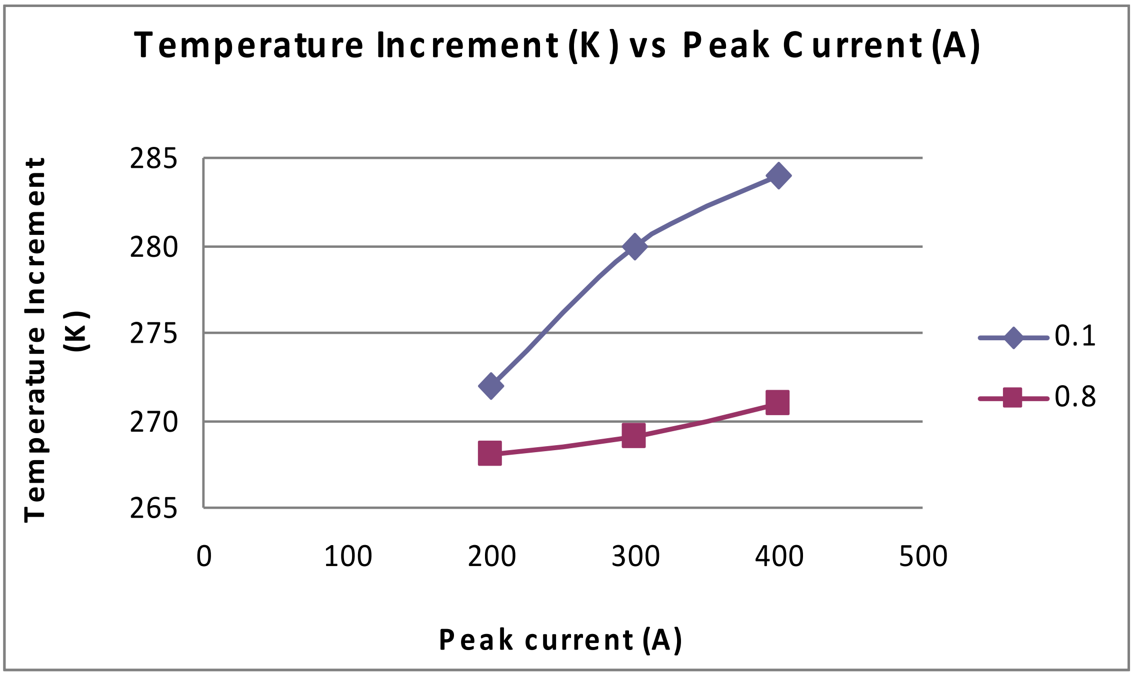

Figure 4.4 Graph of temperature increment vs peak current with different flushing pressure

Figure 4.4 above shows graph of temperature increment versus peak current with presence of different flushing pressure. As the flushing pressure increase from 0.1Mpa to 0.8Mpa, the temperature increment become lower. For example, when current is 300A the temperature is 280K with pressure condition is 0.1Mpa and it reduces to 268K when the pressure is 0.8Mpa. If there is no cooling mechanism at all, the temperature will be much higher and the wire will overheat and breaks. The result of the experiment shows that it is effective to prevent the wire from overheat by flushing the coolant towards the wire.

4.4 EFFECT OF THE KERF ON THE CONVECTIVE COEFFICIENT

Firstly the effect of kerf on the convective coefficient h is experimentally studied. The machining parameters were set as follows. The table shows that whatever value the Ip is set, the experimentally determined value of *h* keeps approximately the same as long as the flushing pressure and the kerf condition are fixed. The table also shows that the coefficient *h* is much larger outside of the kerf than inside of the kerf.

Table 4.6 : The effect of kerf on the convective coefficient

Kerf conditions	Convective coefficient h (W/m^2 K)		
	Ip = 200A	Ip = 300A	Ip = 400A
Inside kerf	17120	18962	19804
Outside kerf	20955	23507	24102

$$h = A\alpha\omega Uo / 2\pi r\beta\,(Uo\text{-}Uo0)$$

$$A = \int Is\,(t^2)dt / ts$$

$$B = Uo / I_P R$$

$$h_{\text{inside kerf}} = \frac{25\,(0.01540)\,(0.0326)\,(1.76)}{2\pi(0.0002)\,(7.3333\text{x}10^{-3})(0.14)}$$

$$= 17\,120\ W/m^2K$$

$$h_{\text{outside kerf}} = \frac{84(0.01540)\,(0.0278)\,(1.50)}{2\pi(0.0002)(6.25\text{x}10^{-3})(0.33)}$$

$$= 20\,955\ W/m^2K$$

Two main causes of wire breakage have been the focus through the experiment. There are poor flushing pressure and an increase in the discharge energy. Poor flushing leads to a lack of dielectric pressure and an increase in discharge energy provokes a higher rate of discharges. Thus, the different types of wire breaking phenomena that have been identified are the following:

i. Sudden increase in energy

In these cases, the wire breakage is provoked by an increase in the discharge frequency. Thus, a reduction in the time interval employed to clean and cool the gap is provoked. As a consequence, a sudden increase in energy appears before wire breakage. The increase in energy is mainly caused by the increase in peak current. This situation could occur when the off-time parameter is reduced too fast under starting conditions.

ii. Successive increases in energy

Wire breakage has been provoked by both the increase in the discharge frequency. In these situations, the energy oscillates until the wire finally breaks. This oscillation appears as a consequence of successive separations and approximations of workpiece and wire. If the corresponding discharges are thoroughly observed, it can be noticed that discharges with high and low ignition delay time appear alternatively . This can be explained by the abrupt oscillating movement of the wire performance.

CHAPTER 5

CONCLUSION AND RECOMMENDATION

5.1 CONCLUSION

Through experiments, the convective heat transfer coefficient in the WEDM process have been estimated. The values of the convective coefficient change with the kerf conditions. When the wire is outside kerf, the temperature is lower thus the coefficient will increase whereas when the wire is inside kerf the temperature is higher and the coefficient will decrease. Wire breakage easily occurred when it is inside kerf because the temperature increment is higher. Temperature becomes one of the factors that lead to wire breakage

The convective coefficient is also very sensitive to the flushing pressure of the coolant. That is why the wire electrode is very easy to break when it has cut deeply into the workpiece during the WEDM process.

Except for the kerf conditions and the flushing pressure, there are many other factors such as wire speed, wire tension, or thickness of workpiece that influence the value of the convective heat transfer coefficient in WEDM process.

For the overall analysis it can concluded that in determining the convective heat transfer coefficient in WEDM , the kerf condition and the flushing pressure plays a significant role in this studies. The more complex geometry of the workpiece, the tendency for the wire to break is easier . If straight cutting and kerf cutting were compared, the wire breakage usually occurred when the kerf cutting is experimented. Larger flushing pressure also helps to prevent the wire from breakage. Increased flushing pressure of the coolant can lower the temperature increment of the wire during WEDM process.

Therefore the larger the flushing pressure is, the larger the coefficient h will be. The results prove that whether the wire is inside kerf or not, the convective coefficient will increase with the increased flushing pressure of the coolant and thus the cooling condition of the WEDM process is ameliorated.

5.2 RECOMMENDATION

This project recommended 2 addition or adjustment in order to make the experiment run more effective.

- Because of the wire breakage easily occurred inside kerf, the convective coefficient inside kerf should be increase as high as possible in order to avoid the frequent wire's breakage.
- In actual machining process, increased flushing pressure of the coolant can ameliorate the cooling conditions of the wire but increase flushing pressure has to be limited to a certain level because very high flushing pressure may cause intensification of the wire's vibration and reduce the machining accuracy

REFERENCES

1. Cheng, G., Han, F. and Feng Z.2007. *Experimental determination of convective heat transfer coefficient in WEDM*

2. Saha, S., Pachon, M. and Ghoshal, A.2005. *Finite element modeling and optimization to prevent breakage in electro-discharge machining.pp 451-463*

3. Banerjee, S., Prasad, B. and Mishra, P.K. 1997. *Analysis of three-dimensional transient heat conduction for predicting wire erosion in the wire electrical discharge machining process, Journal of materials processing technology. pp 134-142*

4. Incropera, F.and De Witt, D. 2005. *Fundamentals of heat transfer.pp 389-412*

5. Tanimura, T., Heuvelman, C.J. and Veenstra, P.C. 2003. *The properties of the servo gap sensor with wire spark erosion machining.pp 59-63*

6. Kinoshita, N., Gamo, G. and Fkui, M.2001.*Control of wire EDM machining electrode from breaking.pp 111-114*

7. Jennes, M., Snoeys, R. and Dekseyer, W.1999.*Comparison of various approaches to model the thermal load on the EDM wire electrode.pp 93-98*

8. Satoshi, T. and Masanori, K.1997. *Measurement of wire electrode temperature in WEDM process.pp 1275-1279*

9. Satoshi, T., Koji, O. and Masanori, K.1997. *Simulation of wire electrode temperature distribution in WEDM.pp 1464-1468*

10. Steve, F., Arthur, R. and Peter, S.2005. *Technology of machine tools*. New York: Mc Graw Hill

11. Gregg, R., Dalton, K. and Richard,R.2004. *Modern materials and manufacturing processes*. New York: Prentice Hall

12. Kuriakose, S. and Shunmugam, M.S.2004.*Characteristics of wire-electro discharge machined Ti6Al4V surface.*

13. Linkbeck, J.R., Williams, M.W. and Wygant, R.M.1990. Manufacturing Technology. *Special Machining Methods : Electrical Discharge Machining. pp 316-318*

14. Mickelson, D.2004. Hard Milling & High Speed Machining : Tool of Change. *Innovative hard machining of forging Die Eliminates EDM. pp 158-162*

APPENDIX A

Figure 6.1 Wire Electro Discharge Machining (WEDM)

Figure 6.2 Milling Machine

APPENDIX B

Figure 6.3 AISI 4140 Steel (Before cutting)

Figure 6.4 AISI 4140 Steel (After cutting)